Nuclear Engineering and Technology 53 (2021) 677–687

Contents lists available at ScienceDirect

Nuclear Engineering and Technology

journal homepage: www.elsevier.com/locate/net

Original Article

Exergetic design and analysis of a nuclear SMR reactor tetrageneration (combined water, heat, power, and chemicals) with designed PCM energy storage and a CO_2 gas turbine inner cycle

Nima Norouzi [a], Maryam Fani [a, *], Saeed Talebi [b]

[a] Energy Engineering and Physics Department, Amirkabir University of Technology, Tehran, Iran
[b] Department of Energy Engineering and Physics, Amirkabir University of Technology (Tehran Polytechnic), 424 Hafez Avenue, PO. Box 15875-4413, Tehran, Iran

ARTICLE INFO

Article history:
Received 31 May 2020
Received in revised form
3 July 2020
Accepted 8 July 2020
Available online 24 July 2020

Keywords:
Solar thermal power plant
Nuclear tetrageneration
Tetrageneration
Exergy
Cogeneration
Nuclear energy storage
Hybrid nuclear system

ABSTRACT

The tendency to renewables is one of the consequences of changing attitudes towards energy issues. As a result, solar energy, which is the leader among renewable energies based on availability and potential, plays a crucial role in full filing global needs. Significant problems with the solar thermal power plants (STPP) are the operation time, which is limited by daylight and is approximately half of the power plants with fossil fuels, and the capital cost. Exergy analysis survey of STPP hybrid with PCM storage carried out using Engineering Equation Solver (EES) program with genetic algorithm (GA) for three different scenarios, based on eight decision variables, which led us to decrease final product cost (electricity) in optimized scenario up to 30% compare to base case scenario from 28.99 $/kWh to 20.27 $/kWh for the case study. Also, in the optimal third scenario of this plant, the inner carbon dioxide gas cycle produces 1200 kW power with a thermal efficiency of 59% and also 1000 m3/h water with an exergy efficiency of 23.4% and 79.70 kg/h with an overall exergy efficiency of 34% is produced in the tetrageneration plant.

1. Introduction

Small modular reactors (SMR) is the bright future of nuclear development. This significant hope is because of the reduced financial risks which allow the countries to meet the ever-growing energy demand using a safe, reliable, and green energy while reducing the carbon footprint of the power sector and helping the climate change mitigation plans [1]. The nuclear plants are complex systems consisted of several subsystems utilizing various resources. Because of this complexity, the thermoeconomic analysis is extremely hard to be examined [2]. Therefore the economic and thermoeconomic analysis cannot provide correct information about the system. However, the thermoeconomic analysis, coupled with the concept of the exergy (second law of thermodynamics), provides a method that reports the cost and quality of the energy (called exergoeconomic analysis) [3]. For a small modular reactor, exergy investigation, physical, chemical, and economic environments must be examined. The physical section incorporates the resources, energy, and the reference environment. The reference environment is the resource that is available to the system limitless and free of expenses. The chemical section is related to the chemical energy, reactions, etc. mainly appear in the reactor or combustion chamber and fuel to energy conversion [4]. The economic section refers to the market, price, investments, and costs. Exergoeconomics or exergetic cost is the exergy required to produce a unit of product; for example, in the energy industry, it is a unit of exergy per kWh of energy. A system can be investigated in the term of its chemical and physical views and modeled in this way, but to optimize the system and its sustainable production economic environment must be considered. A balance needed to be modified between improving efficiency and reducing the costs of a system [1,2]. Some researchers investigated the process of a thermoeconomic analysis on the thermal systems. They stated that this method could be applied to any products generated by the thermal or chemical processes. Then the most important sources of the exergy destruction can be improved to make the overall performance of the plant better to optimize a portion of a system using the exergy analysis [4,5]. Talebi and Norouzi investigated the exergy

* Corresponding author.
E-mail addresses: nima1376@aut.ac.ir (N. Norouzi), mfani@aut.ac.ir (M. Fani), sa.talebi@aut.ac.ir (S. Talebi).

https://doi.org/10.1016/j.net.2020.07.007

analysis method in the PWR nuclear powerplants using a firefly optimization algorithm. This method found to be effective in improving the efficiency of nuclear power plants, and in this research, reactors found to be the main source of the exergy destruction [6]. Norouzi investigated the exergoeconomic analysis in a diesel power plant using the firefly algorithm and optimized the overall process [7,8]. The method found to be effective in the diesel cycle similar to the studies of Talebi and Norouzi and similar to the previous studies in this field the boiler and fuel to energy conversion was the main source of exergy destruction [6]. Prior researches in the SMRs has not developed a detailed exergetic method on the second law analysis of an SMR power plant. This lack of enough information in the literature is the main gap, which is the field in this research. This method requires setting an optimized equilibrium between costs and thermo-hydraulic efficiency to have a financially competitive system [4,9–11].

This paper is aimed to investigate the exergetic balance of an SMR plant to estimate and optimize resources and cost for the system and its subsystems based on the second law of thermodynamics. This paper will examine the exergy concept in the nuclear power plants and nuclear fuels, identify the substantial sources of exergy destruction, and perform an exergy analysis in a 3000 kW SMR system. Also, in this paper, a new tetrageneration plant is proposed and analyzed for the SMR reactors to produce water, power, heat, and chemicals combined in a single plant backed with a PCM energy storage plant.

2. Methodology

2.1. Case study (Shiraz solar thermal plant)

Shiraz solar thermal power plant is located in the south-western part of Iran. The city of Shiraz is one of the Iranian cities with the highest average daily solar radiation and annual hours of sunshine (20 MJ/m^2, and 3000 h, respectively) [11]. The power plant is a pilot power station with a parabolic trough type collector, consist of 48 collectors arranged in 8 rows in North-South direction [9]. The designed and parametric values of the collectors and the nuclear reactor are given in Table 1 [10,11].

The most decisive part of a solar thermal power plant analysis is related to the calculation of reflected radiation by the mirror, concentrated radiation on the beam, and, finally, the absorbed heat by the collector. All of the mentioned parameters depend on situational and geographical parameters such as total radiation (I_o), declination value (δ), incidence angle (θ), zenith angle (θ_z), and geometric factors (R_b). Duffie and Beckman [12–14] introduced the equations to determine the parameters mentioned above, as below Table 2.

Finding out the exact radiation received by the collector and absorbed energy by the collector, both need the calculation of beam radiation. The following equations presented by Ref. [15] will result in the beam radiation amounts. The monthly average of total radiation amounts based on [17] for Shiraz is presented in Table 3. This report indicates that the total annual radiation is 1018.5 W/m^2. In order to have realistic analysis, 12:00 p.m. of September 21st used as calculation base date which ranked 7th among other months' results and also it has irradiation amount near the annual average (958.7 W/m^2) [11].

2.2. Energetic and exergetic analysis of solar system

By having the beam radiation, energy, and exergy received and absorbed by the collector are determined as below Table 4 [1,15,16].

Where i and s indexes represent received and absorbed for both energy and exergy equations, and e refers to energy, while x refers to exergy. The values of the used parameters in equations are summarized in Table 5.

The final purpose of the solar system is to increase the heat transfer to the HTF. Thus, energy and exergy calculation of the beam has a high impact on the total efficiency and final results of solar system performance. Useful energy and exergy transferred to HTF (Q_u, X_u) are determined as below [18–23]. Also, the properties of the HTF are temperature-related, and the total energy and exergy efficiency of the solar system of the Shiraz power plant, consistent with the collector system and receiver system, is presented in Table 4.

2.3. Exergetic improvement by adding PCM storage

The schematic of the working cycle of the 500 kW Shiraz power plant is presented in Fig. 1 [19,20]. The whole cycle is divided into two major parts, the oil cycle, which is the solar part and water cycle, which is a regular steam power generation cycle [17,21]. In the oil cycle, in general, solar radiation is reflected by parabolic mirrors and concentrated on the collector beam, which the heat transfer fluid (HTF) is passing through. This part is consists of the collector field, oil pump, and heat exchangers to transfer the heat to the water cycle. The other side, the water cycle, is just as same as a nuclear steam power generation consisted of an auxiliary nuclear boiler (SMR), steam turbine, condenser, and so forth [18].

Table 1
Parabolic trough collector system specifications [14].

Collector System			
Length (L)	25 m	Mirror Reflectivity (β)	0.873
Width	3.4 m	Cover Transmissivity (τ)	0.96
Aperture (W_0)	3.1 m	Emissivity of cover	0.88
Focal length	88 cm	Receiver Absorptivity (α)	0.94
Receiver Outer diameter (D_o)	42 mm	Collector heat remover factor (FR)	0.98
Receiver Inner diameter (D_i)	125 mm	Intercept factor (Y)	0.93
Cover Outer diameter	70 mm	Concentration ratio (CR)	14
Cover Inner diameter	67 mm	Rim angle	90°
Nuclear system			
Technology	HTGR-I	Outer Cycle	Solar Thermal
Reactor Type	Rapid	Outer Cycle Temp.	550 C
Gen	III & II	Heat transfer	Steam Generator
Working Temp.	750 C	Working fluid II	Oil or water
Working fluid	water	Operation	Primary boiler
Circulation system	2		
Cycle barrier	2		
Inner cycle	Circulator		

Table 2
Solar beam radiation equations.

Description	Equation	
The solar beam declination value	$\delta = 23.45 \sin\left(360\frac{284+n}{365}\right)$	(1)
The solar beam incidence angle	$\cos\theta = \sin\delta \sin\varnothing \cos\beta - \sin\delta \cos\varnothing \sin\beta \cos\gamma + \cos\delta \cos\varnothing \cos\beta \cos\omega + \cos\delta \sin\varnothing \sin\beta \cos\gamma \cos\omega + \cos\delta \sin\beta \sin\gamma \sin\omega$	(2)
The solar beam zenith angle	$\cos\theta_z = \cos\varnothing\cos\delta\cos\omega + \sin\varnothing\sin\delta$	(3)
The solar mirror geometric factors	$R_b = \cos\theta/\cos\theta_z$	(4)
total radiation	$I_b = I_o\left(1 - C_{fa}\right)\left[1 - e^{[-0.0759(\pi/2-\theta_z)]}\right]$	(5)

Table 3
Shiraz monthly average of Total irradiation [20].

W/m^2	month	W/m^2	month
1313.2	July	747.3	January
1170.6	August	907.1	February
958.7	September	1064.8	March
682.5	October	1345.6	April
561.6	November	1475.2	May
581	December	1414.7	June
1018.525			Annual average

The new schematic cycle is shown in Fig. 2, which is a new theoretical sample of Shiraz power plant, integrated with a PCM storage tank to increase both efficiencies and operating time of power plant by preserving excessive solar and nuclear heat gained by the solar field during the working hours [19]. The new arrangement of equipment comes up with this opportunity for the whole power plant to work in different procedures during day and night. The charging cycle, which occurs during the day and night (day: solar activity and night: decrease in the nuclear demand-load), is done when the HTF, which has gained heat passing through the solar field, transfers the water cycle demanded heat via heat exchangers [18,22]. While energy demand is not at its peak or the solar radiation is beyond the power cycle's need, the surplus HTF heat is transferred to PCM storage. In the opposite direction, discharging take place when solar radiation is not adequate or even it is not available anymore. During the discharging cycle, the HTF receives energy from the PCM storage tank. The PCM storage tank will be the primary heat source unless it could not satisfy the energy need, so the auxiliary SMR nuclear boiler will stabilize the HTF to reach the required temperature [1,17,24].

In Ref. [20], all designed and working conditions of the Shiraz STPP cycle are measured and listed. According to Table 6, which is representing temperature, pressure values, and mass flow rate of each process states, the HTF leaving solar field temperature is about 265 °C. Furthermore, according to the results of [12], less difference between the HTF temperature and PCM melting point will result in higher exergetic efficiency of storage. As a result, by having some practical considerations, a commercial PCM melting point of which is 545 °C (LiBr) is used as a case study [24,25].

The supplied exergy by HTF during the charging period, the output exergy at the discharging cycle and exergetic efficiency of PCM storage can be expressed by Equations (25)–(28) from Table 4, where T_0, T_1, T_2, and T_m respectively refer to temperatures of ambient, HTF inlet, HTF outlet, and PCM melting point and storage heat-loss considered to be negligible [17,18,26]. Where C_{HTF} is obtained from Eq. (11) and (m_{HTF}) = 13.7 (kg⁄s). Also, an isothermal PCM melting and negligible sensible heat of PCM is assumed. Moreover, in order to minimize any unsatisfactory conditions, it is assumed that the controlling system would block the storage tank's path as soon as the difference between T_2 and T_m falls below 5 °C [19,27]. The total exergetic outcome of the system with PCM storage is determined as Equation (29), Table 4. Finally, the overall exergetic efficiency of the whole system is measured by dividing the sum of all output exergy to the sum of input exergy of the solar system [20–23,28]. Results showed that using "LiBr" as LHS for Shiraz power plant, due to both PCM physical properties and power plant working conditions, such as HTF temperature, came up with acceptable results shown in Tables 6 and 7.

2.4. Nuclear tetra-generation

Nuclear cogeneration is a mature field of technology, and nuclear power plants have been used for various cogeneration systems such as desalination, heat distribution, etc. but SMR reactors never used for cogeneration and energy storage systems. The previous studies investigating the nuclear-combined heat, power and water production called these systems nuclear trigeneration plants which in this paper authors developed this context into the chemical products such as formic acid which as a hydrogen carrier can be used as energy storage or as a beneficial component in the oil refineries and this system is called nuclear tetrageneration system(combined heat, power, water, and chemical production) (see Fig. 3). Assumptions made for the reverse osmosis and electrochemical reactor plant's operational states are mentioned in Table 8 below.

With the data provided in Table 8, the exergetic model of the nuclear tetrageneration is developed and analyzed in the results and discussion section.

3. Results and discussion

Nowadays, one of the most challenging problems that engineers face are designing systems with high performance, low expenses, and minimum environmental impact. Exergoeconomic is the combination of theory and experiences, which will lead to the optimum point of intersection between the parameters mentioned earlier, and none of the conventional system analysis methods could have results similar to those obtained by exergoeconomic analysis. Expenses refer to the amount of supply and sources consumed to demonstrate any changes made to the cycle flows,

Table 4
Solar beam radiation equations.

description	Equation	
Heat from radiation	$Q_i = (I_b R_b) W_o L N$	(6)
Heat from radiation	$cQ_s = N.I_b.R_b.(\tau\alpha)\left[\beta.Y + \frac{D_o}{W_o - D_o}\right]$	(7)
Exergy received by the collector	$X_i = Q_i[1 - (T_o / T_s)]$	(8)
Exergy received by the collector	$X_s = Q_s[1 - (T_o / T_s)]$	(9)
Thermal conductivity	$K_{HTF} = 0.1882 - 8.304 \times 10^{-5} \times (T_{HTF} + 273.15)$	(10)
Specific Heat	$C_{HTF} = 0.8132 + 3.706 \times 10^{-3} \times (T_{HTF} + 273.15)$	(11)
Density	$\rho_{HTF} = 1071.76 - 0.72 \times (T_{HTF} + 273.15)$	(12)
Prandtl Number	$Pr_{HTF} = 6.73899 + 3.706 \times 10^{21} \times (T_{HTF} + 273.15)^{-7.7127}$	(13)
Heat absorbed by the unit	$Q_u = (W_O - D_O) L.FR\left[\frac{Q_s}{(W_o - D_o)\,L} - \frac{U_O\left(T_{fi} - T_0\right)}{CR}\right]$	(14)
Exergy absorbed by the unit	$X_u = N\,\dot{m}\,\left[\left(h_{fo} - h_{fi}\right) - T_o\left(S_{fo} - S_{fi}\right)\right]$	(15)
Receiver energy efficiency	$\eta_{er} = Q_u / Q_s$	(16)
Receiver exergy efficiency	$\eta_{xr} = X_u / X_s$	(17)
Energy efficiency of the solar collector	$\eta_{ecr} = \eta_c\ \eta_r$	(18)
Exergy efficiency of the solar collector	$\eta_{xcr} = X_u / X_i$	(19)
Energy efficiency of the solar system	$\eta_{ec} = Q_s / Q_i$	(20)
Exergy efficiency of the solar system	$\eta_{er} = Q_u / Q_s$	(21)
Exergy rate	$E = E_{ph} + E_{ch}$	(22)
Chemical Exergy	$E_{ch} = [h(T,\ P) - h(T_0,\ P_0)]\ -\ T_0\ [s\ @(T,\ P) - s\ @(T_0,\ P_0)]$	(23)
Chemical Exergy	$E_{ch} = \sum x_i E_{ch.i}$	(24)
Charging exergy	$X_{pcm.i} = \dot{m}_{HTF}\ C_{HTF}[(T_1 - T_2) - T_0 \ln(T_1 / T_2)]$	(25)
Discharging exergy	$X_{pcm.o} = \dot{m}_{HTF}\ C_{HTF}[(T_2 - T_1) - T_0 \ln(T_2 / T_1)]$	(26)
Charge and Discharge constraint	$T_2 = T_m + (T_1 - T_m)e^{-\left(h_{pcm}A_{pcm} / \dot{m}_{pcm}C_{pcm}\right)}$	(27)
Exergetic PCM storage efficiency	$\eta_{pcm} = X_{pcm.o} / X_{pcm.i}$	(28)
The total exergetic outcome	Total output exergy $= X_u + X_{pcm.o}$	(29)

Table 5
Parametric values for Shiraz power plant.

Parameter	Value	Notes	Reference
n	264	21st September	–
δ	−0.2	Equation (1)	[22]
ϕ	29°36.'	Power plant latitude	–
ω	0	12:00 p.m.	–
θ_z	29.5	Equation (3)	[22]
I_o (W/m^2)	960	Reference	[24]
I_b (W/m^2)	569.83	Equation (5)	[12]
k_T	0.69	Reference	[24]
T_s (K)	5778	Reference	[24]
T_0(°C)	25	Ambient temperature	–
C_{fa}	0.131	Reference	[4]

which will be used as a rational criterion for theoretical calculations. During exergoeconomic analysis, with the assistance of cost balance equations and auxiliary equations, the unit cost of any process stream, either input (fuel) or output (product), is measurable. Also, these equations are the key role players in the optimization of the system from the first stream to the final product by considering economic arrangements.

3.1. Exergy analysis of cycle streams

Exergy is a thermodynamic function defined as maximum available work in a specific thermodynamic condition (pressure, temperature, enthalpy, and so forth.) relative to the reference environment condition and can be used as a measurement of energy quality and quantity. In other words, the exergy can be considered as a measure of the existing nonequilibrium between the discussed matter and the environment [31].

Exergy flow is determined by aggregating the physical and chemical exergy of the flow. The physical exergy (E_{ph}) is the maximum useful work obtained bypassing the unit of mass of a substance of an initial state (T, P) to the environmental state (T_o, P_o) through purely physical processes. Chemical exergy is the maximum useful energy which would be attained by passing from

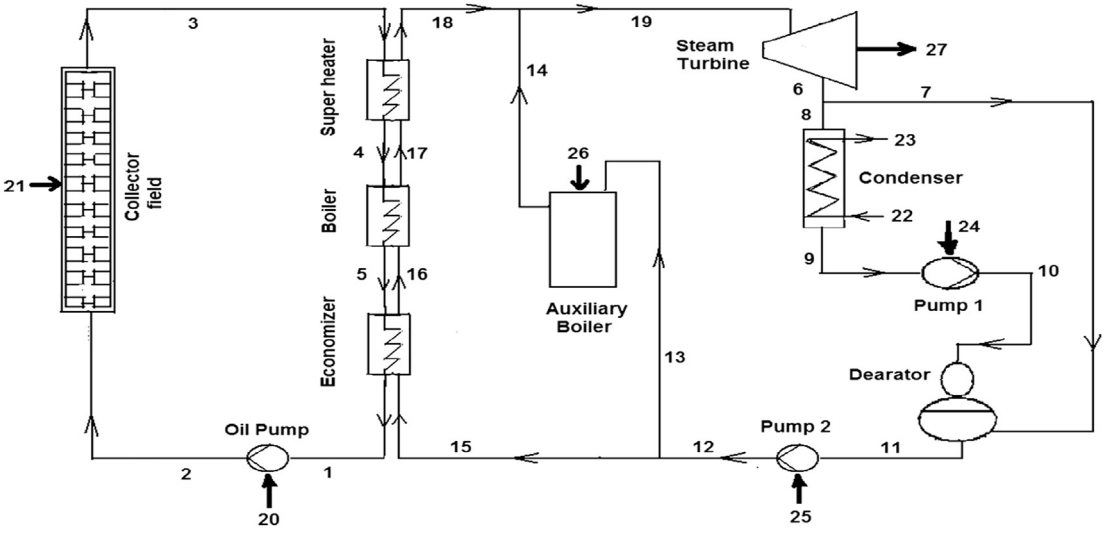

Fig. 1. Schematic diagram of the Shiraz hybrid solar power plant [19].

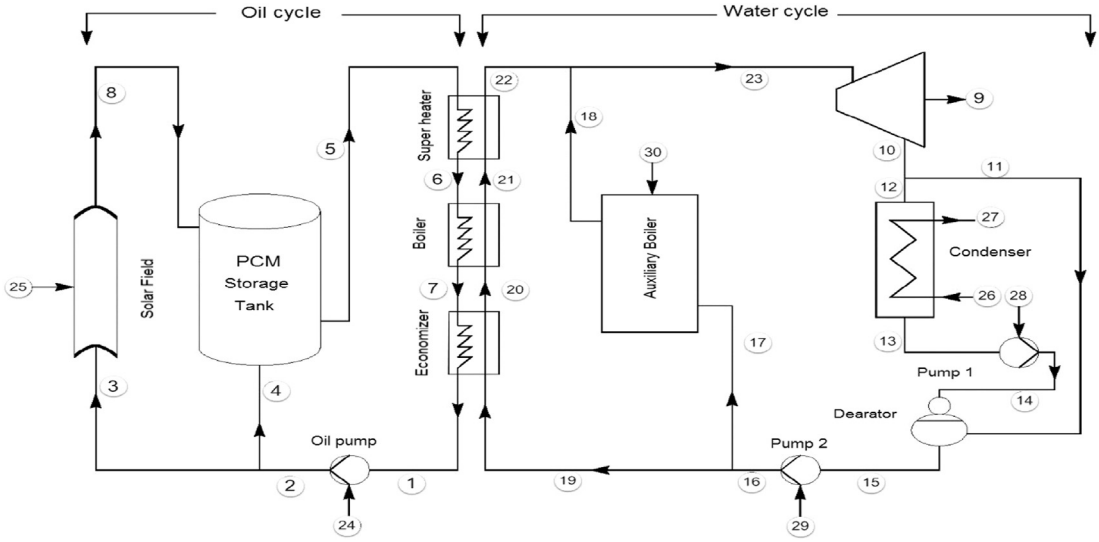

Fig. 2. New schematic diagram of Shiraz solar power plant with PCM storage [29,30].

Table 6
State properties of the system corresponding to Fig. 1 [19,20].

State points	Temperature (K)	Pressure (bar)	Mass kg(s)−1	State points	Temperature (K)	Pressure (bar)	Mass kg(s)−1
1	496.65	2	13.7	12	375.75	21.2	1.7
2	496.65	7.6	13.7	13	375.75	21.2	1
3	538.65	5.05	13.7	14	488.45	21	1
4	536.15	2.82	13.7	15	375.75	21.2	0.7
5	504.15	2.46	13.7	16	488.45	21.1	0.7
6	380.25	1.3	1.7	17	488.45	21.1	0.7
7	380.25	1.3	0.008	18	523.15	21	0.7
8	380.25	1.1	1.7	19	523.15	21	1.7
9	380.25	0.86	1.7	22	298.15	1.013	44.17
10	364.15	1.1	1.7	23	318.15	1.013	44.17
11	375.75	1.1	1.7	26	298.15	20	0.073

Table 7
Selected LHS with LiBr exergetic analysis results [31,32].

Material	Melting point (°C)	Maximum working temperature (°C)	Specific heat (kJ/kg K)	Latent heat (kJ/kg)	Density (kg/m^3)	$X_{pcm,i}$ (W)	$X_{pcm,o}$ (W)	Exergy Loss (W)	Exergetic efficiency (%)
LiBr	545	1265	2.151	3804	3464	111567	95448	16128	85.54

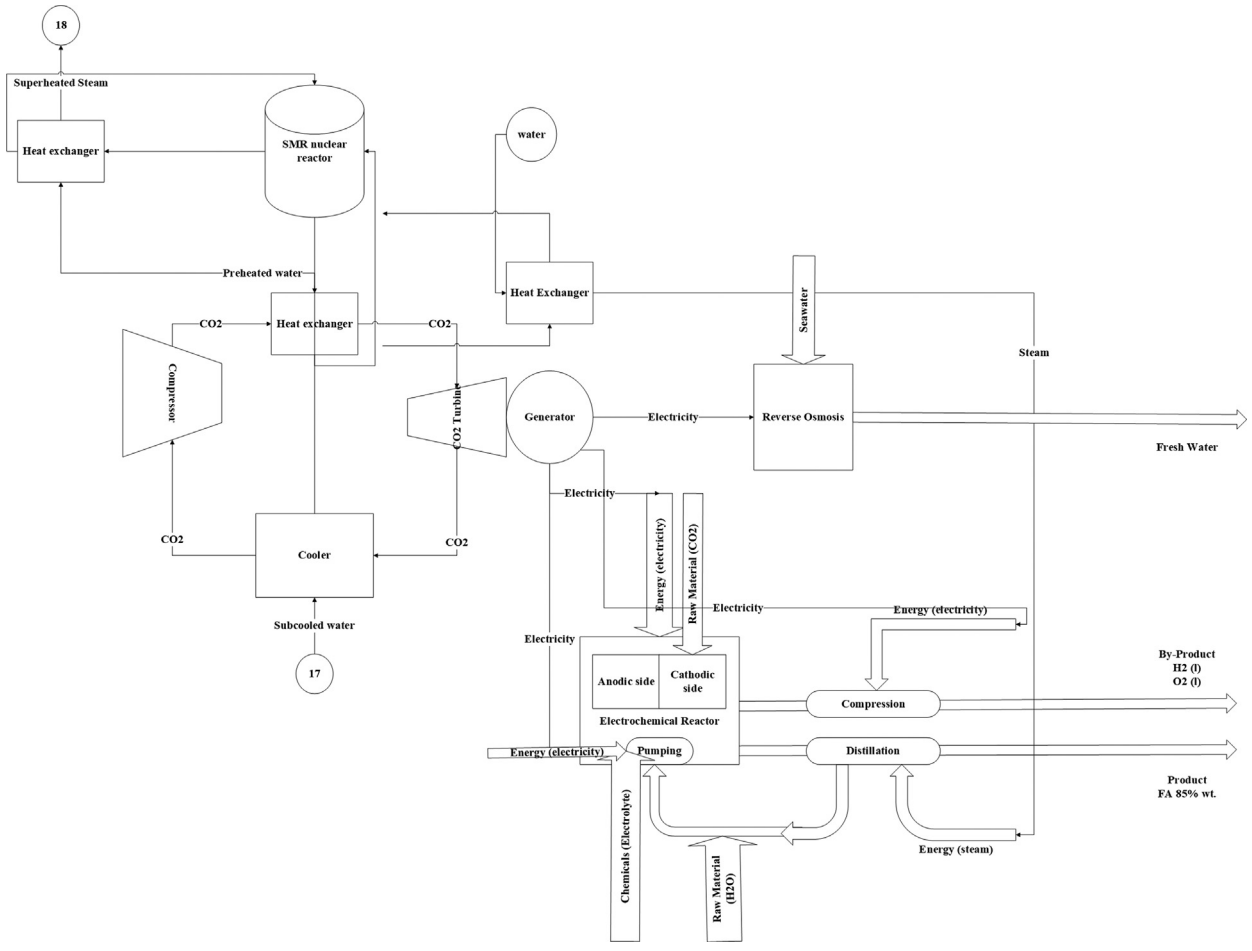

Fig. 3. Nuclear inner cycle and tetra-generation plant (state 17 to 18 from Figs. 1 and 2).

the environmental state to the dead state, using chemical processes with reactants and products at the environmental temperature and pressure, while the composition is not in chemical equilibrium with the environment. The precise and detailed calculation method for exergy equations is provided in Refs. [32], but in general, the basic exergy equation areas mentioned in Table 4.

The new theoretical and schematic cycle of the Shiraz power plant with PCM storage with the new arrangement and numbering

Table 8
Assumptions made for the reverse osmosis and electrochemical reactor plant's operational states.

Assumption (3000 KW SMR reactor)	Value
Reverse Osmosis	
Water production	24000 m^3/day
SEC	0.7 kWh/m^3
Recovery factor	60%
Seawater consumption	40000 m^3/day
Salinity	1098 ppm
Pressure 1st pass	9.22 atm
Pressure 2nd pass	9.832 atm
Temperature	25 C
Electrochemical reactor	
Formic acid production	79.70 kg/h
carbon capture	75.20 kg/h
power penalty	376.38 kWh/time (1 h)
Total efficiency	44%
investment cost	7.2 M$
Cathode	Sn NPs
Anode	IrO_2

has been shown in Fig. 2 and based on the stream exergy equations determined above, the exergy of every stream is calculated and is expressed in Table 9.

In Table 9, that illustrates the power plant cycle, and it is deemed to have different paths for streams in day and night. Thus, there would be different exergy amounts, and also the exergoeconomic equations should consist of both of the parameters. Indeed, the exergoeconomic analysis should strike a balance between day and night parameters, such as operating time during the day and night, storage system capacity, and so forth (Table 10). The results of all the equations in the exergy analysis section are presented in Table 11.

3.2. Numerical results and discussion

Regarding equations and values expressed in the methodology, the base case of existing Shiraz power plant costs is available with 30-equations, 30-unknowns simple calculations. However, optimization needs more considerations. Allocating the constraints amount in lieu of the fixed value for the critical parameters of the problem is the first step to find out the best operating point of the system. Engineering equation solver (EES) as a robust and user-friendly program with extensive thermodynamic parameters and values database is used to optimize the results. Two different exergoeconomic problems have been modeled; first, Shiraz solar power plant hybrid with LHS (PCM) and second, the optimized results of the problem above. Eight decision variables with their reasonable bounds are given in Table 12. Based on the expressed limitations by using the Genetic Algorithm, optimization results came up with up to 10% reduction in final product cost.

To be well performed, the genetic algorithm requires some input parameters to be set up correctly. The user should specify the following items, such as the reasonable range of variables, the sample size of the initial population of parent individuals, the scaling factor, and the maximum number of generations of offspring [36]. Parameters' values are used as follows in Table 13.

Exergoeconomic optimization results compared with two other scenarios, Shiraz power plant existing cycle and hybrid Shiraz power plant with LHS storage, are listed in Table 14, which shows significant improvement in cost reduction.

Table 9
Cycle streams' calculated exergy corresponding to Fig. 2.

State points	Mass	Exergy	State points	Mass	Exergy
	(Kg/s)	(MW)		(Kg/s)	(MW)
1	13.7	5.86	12	1.7	3.95
2	13.7	5.86	13	1.7	0.564
3	13.7	5.86	14	1.7	0.508
4	13.7	0.1116	15	1.7	0.527
5	13.7	7.592 (day)/6.795 (night)	16	1.7	0.538
6	13.7	7.504 (day)/6.707 (night)	17	1	0.317
7	13.7	6.095 (day)/5.298 (night)	18	1	2.64
8	1.7	7.701	19	0.7	0.221
9	–	0.5	20	0.7	0.535
10	1.7	3.97	21	0.7	1.78
11	0.008	0.019	22	0.7	1.85
12	1.7	3.95	23	1.7	4.5
13	1.7	0.564	26	44.17	0
14	1.7	0.508	27	44.17	3.39
15	1.7	0.527	30	0.073	3.76

3.3. Generalization survey

Another investigation has been carried out by applying the designed conditions to 250 kW, 1000 kW, and 2000 kW STTPs, which confirmed the enormous impact of LHS on final product cost to obtain practical results from the current study. The results are shown in Table 15 and Fig. 4. All 4 cases are optimized and hybrid with a PCM storage tank and nuclear SMR system.

As it is expected, higher power output comes with lower final product cost, because doubling the power plant capacity, does not result in doubling the capital cost while capital cost of STTP is the most crucial parameter in STTPs' economic issues.

The lowest exergetic efficiency is related to the solar field and collector system, with only 56%. Therefore, it seems to be very beneficial and productive to enhance solar system performance. Because solar energy is available free of charge, by increasing energy demand and energy cost, utilizing renewable energies as much as possible would be the only solution for the future (see Fig. 5).

Condenser's primary objective is to gain heat from steam leaving the steam turbine and transfer it to the environment in different ways, depending on the condenser type. Base on the results from Table 14, the exergetic efficiency of the condenser is acceptable (84%) which means that the component is functioning correctly, but the prominent point is that about 2.8 (MW) exergy is being thrown away while every bit of this energy would help to achieve better results.

Shiraz solar thermal power plant has a great response to adding an LHS system filled with PCM material and a nuclear-coupled reactor. The results showed that by adding a storage tank and nuclear-coupled reactor to the power plant cycle, the electricity production cost would be reduced up to 22.3%. Furthermore, exergoeconomic analysis helped to decrease more than 10% of electricity cost to achieve the goal of final cost reduction up to 32% from power plant existing regular cycle by optimizing and adding PCM storage tank and nuclear-coupled reactor.

According to Table 15 and Fig. 4, the final product cost for an STTP hybrid with LHS decreases by increasing the power plant's output power, but it cannot be generalized to all cases and capacities. Indeed this result is obtained using Shiraz STTP information, and a complete parametric survey is needed to determine the exact optimum capacity and conditions. This phenomenon arises from the low efficiency of the solar collectors' system, which is discussed in the exergy part of the paper in detail (see Fig. 6).

3.4. Exergy analysis of the nuclear tetrageneration plant

The second law of thermodynamics results of the nuclear tetrageneration plant is summarized in the following Table 16. The

Table 10
Energy analysis results of collector, receiver and solar system.

System	Received Energy (kW)	Transferred Energy (kW)	Energy Loss (kW)	Energy Loss (%)	First Law Efficiency (%)
Collector	$Q_i = 487.5$	$Q_s = 223.4$	$Q_l = 264.1$	54.17	45.82
Receiver	$Q_s = 223.4$	$Q_u = 151.7$	$Q_l = 71.7$	32.1	67.9
Solar system (total)	$Q_i = 487.5$	$Q_u = 151.7$	$Q_l = 335.8$	68.88	31.11

Table 11
Exergy analysis results of Collector, Receiver and Solar system.

System	Received Exergy (kW)	Transferred Exergy (kW)	Exergy Loss = irreversibility (kW)	Exergy Loss (%)	Second Law Efficiency (%)
Collector	$X_i = 458.2$	$X_s = 89.3$	$X_l = 368.9$	80.51	19.48
Receiver	$X_s = 89.3$	$X_u = 47.1$	$X_l = 42.2$	47.25	52.74
Solar system (total)	$X_i = 458.2$	$X_u = 47.1$	$X_l = 411.1$	89.72	10.27

Table 12
Decision variables range for exergoeconomic optimization.

Variable and range
$0.4 \leq \eta_{Oil\ pump} \leq 0.6$
$0.45 \leq \eta_{Pump\ 1} \leq 0.6$
$0.45 \leq \eta_{Pump\ 2} \leq 0.6$
$513.15\ K \leq T_{23} \leq 533.15\ K$
$18\ bar \leq P_{23} \leq 24\ bar$
$12\ kg/s \leq \dot{m}_{HTF} \leq 14\ kg/s$
$0.5 \leq$ ***Day shift*** / ***Total working hours*** ≤ 0.65
$0.35 \leq$ ***Night shift*** / ***Total working hours*** ≤ 0.56

Table 13
Genetic algorithm parameters.

Parameters	Value
Population size	100
Maximum generation number	100
Elite children population	4
Selection process	Stochastic uniform
Crossover fraction	50%

results in this plant are divided into three subsections of chemical production, power generation, and water desalination. Every three subsections are analyzed exergetically in Table 16.

Table 16 demonstrates the exergy analysis results of the RO desalination plant. The result shows the importance of incorporating an energy recovery device in the hydraulic turbine, which through recovering the pressure from the rejected disposal water, can improve its exergy efficiency from 23.4% to 27.3%, as shown in Fig. 7.

Moreover, this analysis shows that the highest exergy destruction to produce drinking water and for irrigation occurs in the rejected water, and lowest occurs in the permeate flow rate, accounting 53.2% for 2.1%, respectively. The second highest exergy destruction occurs in the pump, which is approximately 25.4%, and the third one occurs in the same in the membrane, as shown in Fig. 8.

The outputs of the thermodynamic analysis by taking the 1st and 2nd law of thermodynamics efficiencies into account demonstrate that the storage efficiency of the formic acid as a solar fuel is not as efficient as the batteries. However, solar fuel storage capacity is much higher and flexible. The battery storage capacity is on the scale of hundreds of kilowatt-hours, but the chemical solar fuel storage is as capable as hundreds of megawatt-hours (see Table 16).

The exergy and energy analysis used in this section to determine the exergy and energy efficiency of the electrochemical process that can be mentioned as a chemical storage plant. In this section, the exergy and energy efficiency is calculated for each anodic option in the term of the charging and discharging processes of the storage system. The exergy analysis is more accurate than the energy analysis in the field sustainability. The results show that the exergy

Table 14
Results and cost comparison between 3 scenarios for Shiraz STTP.

Variable	Original cycle without LHS	Original cycle with LHS storage and nuclear unit	Optimized cycle with LHS storage and nuclear unit
$\eta_{Oil\ pump}$	0.45	0.45	0.6
$\eta_{Pump\ 1}$	0.5	0.5	0.46
$\eta_{Pump\ 2}$	0.55	0.55	0.49
T_{23} (k)	523.15	523.15	513.3
P_{23} (bar)	21	21	24
$\dot{m}_{HTF}$ (kg/s)	13.7	13.7	14.88
Total operating hours	1250	2500	2500
Day shift / **Total operating hours**	1	0.65	0.58
Night shift / **Total operating hours**	0	0.35	0.58
Final product cost ($/kWh)	0.2899	0.2253	0.2027

Table 15
Comparison between optimized 250 kW, 500 kW, 1000 kW, and 2000 kW STTPs.

Variable	250 kW	500 kW	1000 kW	2000 kW
$\eta_{Oil\ pump}$	0.57	0.6	0.59	0.55
$\eta_{Pump\ 1}$	0.54	0.46	0.49	0.51
$\eta_{Pump\ 2}$	0.51	0.49	0.51	0.56
T_{23} (k)	523.15	513.3	513.4	514
P_{23} (bar)	21	24	23.5	23.86
$\dot{m}_{HTF}$ (kg/s)	13.23	14.88	12.53	14.96
Total operating hours	2500	2500	2500	2500
Day shift / Total operating hours	0.5	0.5	0.5	0.5
Night shift / Total operating hours	0.5	0.5	0.5	0.5
Final product cost ($/kWh)	0.3204	0.2027	0.1408	0.111

Table 16
Exergy analysis of the nuclear tetrageneration plant.

Parameter	Value
Reverse Osmosis	
Exergy efficiency	23.4%
Recovery	60%
Exergy rate	955.6 kW
Exergy destruction	732 kW
Water production	1000 m^3/h
Electrochemical reactor	
Formic acid production	79.70 kg/h
Energy cost	0.16 $/kWh-product
Exergy rate cost	0.21 $/kWh exergy
Exergy efficiency	34%
CO_2 gas turbine cycle	
power production	1200 kW
Energy efficiency	58.6%
Exergy efficiency	59.3%

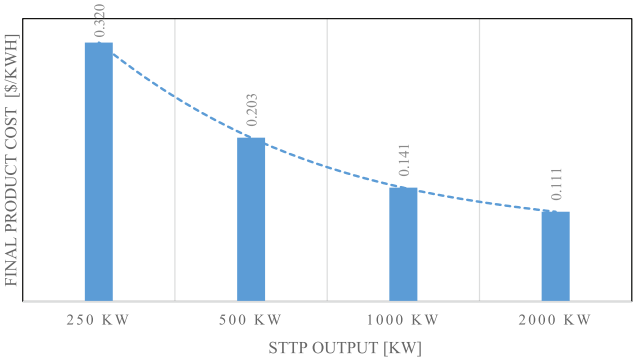

Fig. 4. Power plant exergetic efficiency with and without LHS.

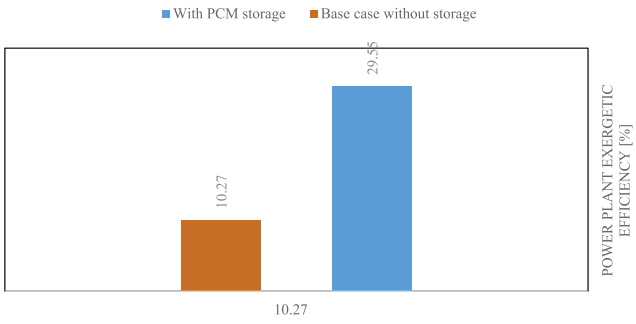

Fig. 5. Shiraz STTP exergetic efficiency with and without LHS.

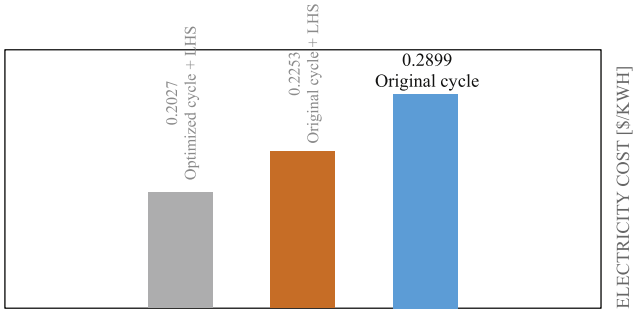

Fig. 6. Electricity cost comparison between 3 scenarios for Shiraz STTP.

efficiency of the electrochemical reduction process based chemical storage units is in a range of 35–45% (conventionally). Norouzi calculated the exergy performances of the typical energy storage plants in their research. They noted that the average exergy performance of the thermal energy storage systems is in a range of 22–35%, and this amount for battery storage is more than 94% [33]. The results for the electrochemical reduction show that the exergy performance of this system is much higher than the thermal storage and less than the batteries. However, the capacity of the batteries is on a KW scale and cannot be compared with the MW and GW scales of the thermal and chemical storages [34–36].

4. Conclusion

Hybrid Solar thermal and nuclear power plant with LHS (PCM) is the solution to the STTPs' issue of much lower operating hours (2500 h a year), while the operating time can be increased up to 8400 h per year, similar to the other types of power plants using fossil fuels or nuclear power plants. The standard solar power plants' operating time varies from time to time and location. However, adding storage tanks and nuclear reactors with suitable capacity can extend the working hours to 3 times the base case (2500–8400 in this paper). Among the solar field components, the collector system has the most exergy lost value, which is more than half the value of transferred exergy amount to the component. As a result, the overall solar field exergetic efficiency became about 30%, which is not very acceptable, and it would be beneficial to strive for better results. It has been conducted that by adding appropriate PCM and an SMR nuclear boiler, compatible with power plant conditions will result in considerable improvement in overall exergetic efficiency. For the case study of the Shiraz thermal power plant, the difference between the base case without storage and nuclear couplings and with the storage system filled with selected PCM is more than 19%. Also, in this plant, the carbon dioxide cycle produces 1200 kW power with a thermal efficiency of 59% and also 1000 m^3/h water with an exergy efficiency of 23.4% and 79.70 kg/h with an overall exergy efficiency of 34% is produced in the tetrageneration plant.

Declaration of competing interest

The authors declare that they have no known competing financial interests or personal relationships that could have appeared to influence the work reported in this paper.

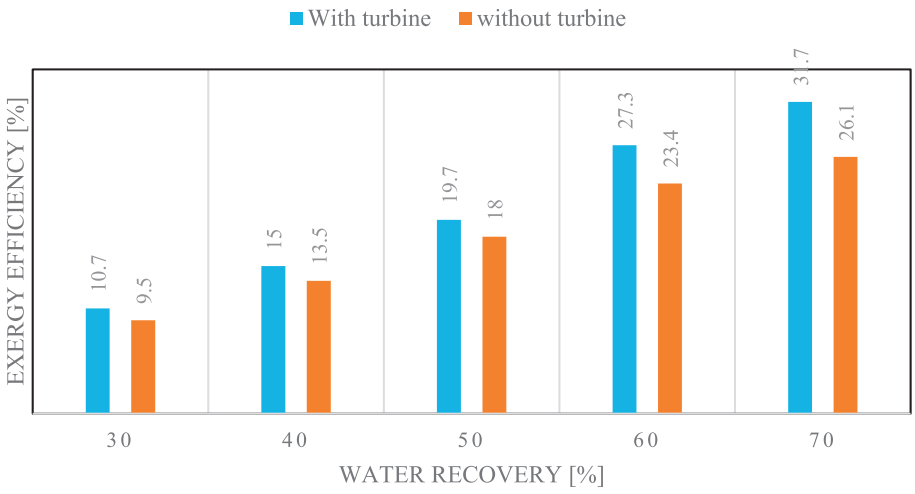

Fig. 7. Exergy efficiency in the reverse osmosis section of the nuclear tetrageneration.

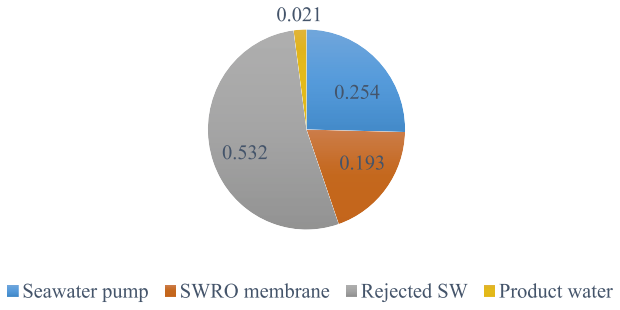

Fig. 8. Share of each component from the exergy destruction in the water production plant.

Appendix A. Supplementary data

Supplementary data to this article can be found online at https://doi.org/10.1016/j.net.2020.07.007.

References

[1] U. Pelay, L. Luo, Y. Fan, D. Stitou, M. Rood, Thermal energy storage systems for concentrated solar power plants, Renew. Sustain. Energy Rev. 79 (2017) 82–100.
[2] K. Karunamurthy, M.R. Rajesh, B. Vijaypal, A. Kumar, Thermal Conductivity and Charging & Discharging Characteristics of a Thermal Energy Storage System Blended with Al_2O_3 Nanoparticles, Nano Hybrids and Composites, Trans Tech Publ, 2017.
[3] J. Yang, L.-S. Tang, R.-Y. Bao, L. Bai, Z.-Y. Liu, W. Yang, Largely enhanced thermal conductivity of poly (ethylene glycol)/boron nitride composite phase change materials for solar-thermal-electric energy conversion and storage with very low content of graphene nanoplatelets, Chem. Eng. J. 315 (2017) 481–490.
[4] Y. Addad, M. Abutayeh, E. Abu-Nada, Effects of nanofluids on the performance of a PCM-based thermal energy storage system, J. Energy Eng. 143 (2017), 04017006.
[5] B. Xu, P. Li, C. Chan, E. Tumilowicz, General volume sizing strategy for thermal storage system using phase change material for concentrated solar thermal power plant, Appl. Energy 140 (2015) 256–268.
[6] M. Seitz, M. Johnson, S. Hübner, Economic impact of latent heat thermal energy storage systems within direct steam generating solar thermal power plants with parabolic troughs, Energy Convers. Manag. 143 (2017) 286–294.
[7] S. Talebi, N. Norouzi, Entropy and exergy analysis and optimization of the VVER nuclear power plant with a capacity of 1000 MW using the firefly optimization algorithm, Nucl. Eng Technol. (2020), https://doi.org/10.1016/j.net.2020.05.011. In press.
[8] H.-S. Park, T.-S. Kwon, S.-K. Moon, S. Cho, D.-J. Euh, S.-J. Yi, Contribution of thermal–hydraulic validation tests to the standard design approval of SMART, Nucl. Eng. Technol. 49 (2017) 1537–1546, https://doi.org/10.1016/j.net.2017.06.009.
[9] A.A.E. Abdelhameed, K.S. Chaudri, Y. Kim, Three-D core multiphysics for simulating passively autonomous power maneuvering in soluble-boron-free SMR with helical steam generator, Nucl. Eng. Technol. (2020), https://doi.org/10.1016/j.net.2020.05.009. In press.
[10] P. Zhao, Z. Liu, T. Yu, J. Xie, Z. Chen, C. Shen, Code development on steady-state thermal-hydraulic for Small Modular Natural circulation lead-based fast reactor, Nucl. Eng. Technol. (2020), https://doi.org/10.1016/j.net.2020.05.023. In press.
[11] M. Ilyas, F. Aydogan, Steam generator performance improvements for integral small modular reactors, Nucl. Eng. Technol. 49 (2017) 1669–1679, https://doi.org/10.1016/j.net.2017.08.011.
[12] S.A. Alameri, J.C. King, A.K. Alkaabi, Y. Addad, Prismatic-core advanced high temperature reactor and thermal energy storage coupled system – a preliminary design, Nucl. Eng. Technol. 52 (2020) 248–257, https://doi.org/10.1016/j.net.2019.07.028.
[13] F. Chavagnat, D. Curtis, Initial estimates of the economical attractiveness of a nuclear closed Brayton combined cycle operating with firebrick resistance-heated energy storage, Nucl. Eng. Technol. 50 (2018) 488–493, https://doi.org/10.1016/j.net.2017.11.011.
[14] R. Jacob, M. Belusko, A.I. Fernández, L.F. Cabeza, W. Saman, F. Bruno, Embodied energy and cost of high temperature thermal energy storage systems for use with concentrated solar power plants, Appl. Energy 180 (2016) 586–597.
[15] G. Comodi, F. Carducci, J.Y. Sze, N. Balamurugan, A. Romagnoli, Storing energy for cooling demand management in tropical climates: a techno-economic comparison between different energy storage technologies, Energy 121 (2017) 676–694.
[16] M.H. Mahfuz, A. Kamyar, O. Afshar, M. Sarraf, M.R. Anisur, M.A. Kibria, et al., Exergetic analysis of a solar thermal power system with PCM storage, Energy Convers. Manag. 78 (2014) 486–492.
[17] D. Mazzeo, G. Oliveti, Parametric study and approximation of the exact analytical solution of the Stefan problem in a finite PCM layer in a steady periodic regime, Int. Commun. Heat Mass Tran. 84 (2017) 49–65.
[18] A. Baghernejad, M. Yaghoubi, Thermoeconomic methodology for analysis and optimization of a hybrid solar thermal power plant, Int. J. Green Energy 10 (2013) 588–609.
[19] J.A. Duffie, W.A. Beckman, Solar Engineering of Thermal Processes, fourth ed., 2013.
[20] M. Romero, J. González-Aguilar, Solar thermal power plants: from, in: K.R. Rao (Ed.), Endangered Species to Bulk Power Production in Sun-Belt Regions, Energy & Power Generation Handbook, ASME, New York, 2011.
[21] M. Rezaei, M. Anisur, M. Mahfuz, M. Kibria, R. Saidur, I. Metselaar, Performance and cost analysis of phase change materials with different melting temperatures in heating systems, Energy 53 (2013) 173–178.
[22] [28] Y.-Q. Li, Y.-L. He, Z.-F. Wang, C. Xu, W. Wang, Exergy analysis of two phase change materials storage system for solar thermal power with finite-time thermodynamics, Renew. Energy 39 (2012) 447–454.
[23] C.W. Robak, T.L. Bergman, A. Faghri, Economic evaluation of latent heat thermal energy storage using embedded thermosyphons for concentrating solar power applications, Sol. Energy 85 (2011) 2461–2473.
[24] E. Querol, B. Gonzalez-Regueral, J.L. Perez-Benedito, Practical Approach to Exergy and Thermoeconomic Analyses of Industrial Processes, Springer Science & Business Media, 2012.
[25] I. Dincer, M.A. Rosen, P. Ahmadi, Optimization of Energy Systems, Wiley, 2017.
[26] M. Rahmatian, F. Ahmadi Boyaghchi, Exergo-environmental and exergo-economic analyses and multi-criteria optimization of a novel solar-driven CCHP based on Kalina cycle, Energy Equip. Syst. 4 (2016) 225–244.
[27] A. Naserbegi, M. Aghaie, A. Minuchehr, Gh Alahyarizadeh, A novel exergy

optimization of Bushehr nuclear power plant by gravitational search algorithm (GSA), Energy 148 (2018) 373–385.
[28] Z. Yang, Z. Meng, C. Yan, K. Chen, Heat transfer and flow characteristics of a cooling thimble in a molten salt reactor residual heat removal system, Nucl. Eng. Technol. 49 (2017) 1617–1628.
[29] J. Moon, Y.H. Jeong, Y. Addad, Design of air-cooled waste heat removal system with string type direct contact heat exchanger and investigation of oil film instability, Nucl. Eng. Technol. 52 (2020) 734–741.
[30] A.D. Ronco, A. Cammi, S. Lorenzi, Preliminary analysis and design of the heat exchangers for the molten salt fast reactor, Nucl. Eng. Technol. 52 (2020) 51–58.
[31] Z. Yuan, K.E. Herold, Specific heat measurements on aqueous lithium bromide, HVAC R Res. 11 (2005) 361–375, 2005.
[32] N. Norouzi, 4E Analysis and design of a combined cycle with a geothermal condensing system in Iranian Moghan diesel power plant, Int. J. Air-Conditioning Refrig. (2020), https://doi.org/10.1142/S2010132520500224. In press.
[33] N. Norouzi, S. Talebi, M. Fabi, H. Khajehpour, Heavy oil thermal conversion and refinement to the green petroleum: a petrochemical refinement plant using the sustainable formic acid for the process, Biointerface Res. Appl. Chem. 10 (2020) 6088–6100, https://doi.org/10.33263/BRIAC105.60886100.
[34] N. Norouzi, 4E analysis of a fuel cell and gas turbine hybrid energy system, Biointerface Res. Appl. Chem. 11 (2021) 7568–7579, https://doi.org/10.33263/BRIAC111.75687579.
[35] J.S. Akhatov, Energy and exergy analysis of solar PV powered reverse osmosis desalination, Appl. Sol. Energy 52 (2016) 265–270, https://doi.org/10.3103/S0003701X16040034.
[36] N. Norouzi, G. Zarazua de Rubens, S. Choupanpiesheh, P. Enevoldsen, When pandemics impact economies and climate change: exploring the impacts of COVID-19 on oil and electricity demand in China, Energy Res. Soc. Sci. 68 (2020), https://doi.org/10.1016/j.erss.2020.101654, 101654.